

# Hebbian Physics Networks: A Self-Organizing Computational Architecture Based on Local Physical Laws

Gunjan Auti\* and Hirofumi Daiguji

*Department of Mechanical Engineering, The University of Tokyo, Tokyo, Japan*

Gouhei Tanaka

*Graduate School of Engineering, Nagoya Institute of Technology, Japan and  
International Research Center for Neurointelligence, The University of Tokyo, Japan*

Physical transport processes organize through local interactions that redistribute imbalance while preserving conservation. Classical solvers enforce this organization by applying fixed discrete operators on rigid grids. We introduce the Hebbian Physics Network (HPN), a computational framework that replaces this rigid scaffolding with a plastic transport geometry. An HPN is a coupled dynamical system of physical states on nodes and constitutive weights on edges in a graph. Residuals—local violations of continuity, momentum balance, or energy conservation—act as thermodynamic forces that drive the joint evolution of both the state and the operator (i.e. the adaptive weights). The weights adapt through a three-factor Hebbian rule, which we prove constitutes a strictly local gradient descent on the residual energy. This mechanism ensures thermodynamic stability: near equilibrium, the learned operator naturally converges to a symmetric, positive-definite form, rigorously reproducing Onsager’s reciprocal relations without explicit enforcement. Far from equilibrium, the system undergoes a self-organizing search for a transport topology that restores global coercivity. Unlike optimization-based approaches that impose physics through global loss functions, HPNs embed conservation intrinsically: transport is restored locally by the evolving operator itself, without a global Poisson solve or backpropagated objective. We demonstrate the framework on scalar diffusion and incompressible lid-driven cavity flow, showing that physically consistent transport geometries and flow structures emerge from random initial conditions solely through residual-driven local adaptation. HPNs thus reframe computation not as the solution of a fixed equation, but as a thermodynamic relaxation process where the constitutive geometry and physical state co-evolve.

## I. INTRODUCTION

The central abstraction of classical computational physics is the separation of state and structure. In a conventional simulation, the physical state—whether velocity, temperature, or concentration—evolves dynamically, but the geometric structure that governs its transport is frozen at the outset. Whether defined by a finite difference stencil, a finite element stiffness matrix, or a connection graph, the discretized constitutive operator is treated as a rigid scaffolding. It dictates strictly how fluxes propagate and how nodes influence one another, regardless of the evolving flow. Classical time-stepping schemes then enforce conservation by repeatedly applying this fixed operator under a global synchronizing clock, forcing the system to conform to a pre-determined geometric constraint [1–3].

However, in non-equilibrium thermodynamics, the structure of transport is rarely static. Nature does not impose a fixed grid; it evolves pathways in response to thermodynamic stresses. Onsager’s reciprocal theory [4, 5] identifies the symmetric, positive operator linking thermodynamic forces to fluxes as the local geometric structure governing dissipation. Prigogine’s theory of far-from-equilibrium systems [6, 7] extends this, suggesting that conservation is sustained through continual local

adjustments of these force–flux couplings, not by global coordination. In this perspective, the “constitutive operator”—the map between force and flux—is not a constant background, but a dynamic field that co-evolves with the state variables to maximize entropy production.

Building on this thermodynamic picture, we introduce the Hebbian Physics Network (HPN), a computational framework that replaces the rigid scaffolding of classical solvers with a plastic transport geometry.

In an HPN, the discrete operator is not prescribed; it is treated as a physical degree of freedom that relaxes alongside the state. The network is defined on a discrete graph whose nodes store physical state variables ( $U$ ) and whose directed edges represent the pathways along which flux can flow. Each directed edge  $j \rightarrow i$  carries a coupling weight  $W_{ij}$  that determines how the state at node  $j$  contributes to the flux entering node  $i$  (see Fig. 1). These weights collectively form the local geometric structure of the graph: they specify which transport pathways are available and how strongly they interact.

To drive the adaptation of this geometry, we identify the local imbalance measured internally by the network. For each node  $i$ , we compute a residual:

$$R_i = \sum_j J_{ij} = \sum_j W_{ij} U_j. \quad (1)$$

In standard numerical methods, this residual is viewed as a numerical error to be annihilated by a global solver.

---

\* [gunjanauti@thml.t.u-tokyo.ac.jp](mailto:gunjanauti@thml.t.u-tokyo.ac.jp)

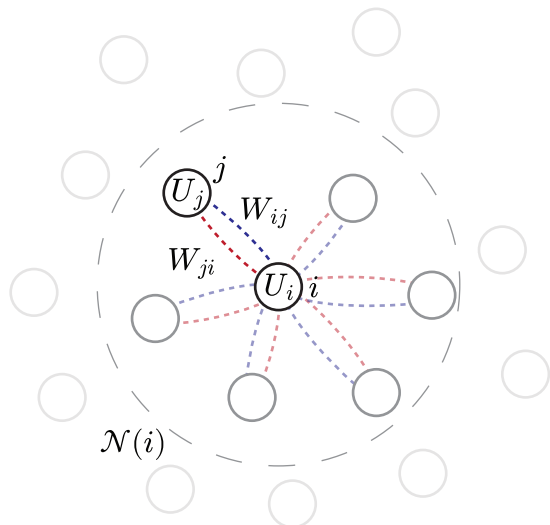


FIG. 1. **Schematic of the graph  $\mathcal{G}$** : each node  $i$  interacts with its neighbors  $j \in \mathcal{N}(i)$  through directed couplings  $W_{ij}$ ; reciprocal edges  $j \rightarrow i$  carry distinct couplings  $W_{ji}$ .  $U_i$  and  $U_j$  are the state variables at nodes  $i$  and  $j$ , respectively.

In the HPN framework, we interpret residual  $R_i$  as a physical accumulation of the conserved quantity (e.g., mass or momentum) at node  $i$  as shown in Eq (1). This accumulation creates a local stress that acts upon the incident edges. It quantifies a local deviation whose relaxation requires modifying the force-flux mapping—precisely the form of adjustment emphasized in non-equilibrium thermodynamics. Thus,  $R_i$  provides the natural thermodynamic signal governing the evolution of the constitutive operator. The evolution of the network follows a principle of constitutive relaxation: if a conserved quantity accumulates at a node, the incident pathways ‘yield’ (increasing their effective conductance) to relieve the stress, while pathways that oppose relaxation are suppressed. This dynamic reshaping of the local transport geometry ensures that the network evolves toward a configuration where conservation is satisfied intrinsically. This mechanism is formalized as a three-factor Hebbian rule in neuro-modulated form [8, 9]:

$$\Delta W_{ij} = -\eta_p f(R_i) U_j - \lambda W_{ij}, \quad (2)$$

where the three factors are: (i) an eligibility signal  $e_{ij} = U_j$  (pre-activity) is gated by (ii) a modulatory factor  $m_i = f(R_i)$  derived from the residual, with (iii)  $\lambda$  providing homeostatic decay. An additional promoter term ( $+\varepsilon g(R_i)$ ) can be included to have a finite conductance for each edge. While Hebbian in algebraic form, the update is causal in mechanism: updates respond to the instantaneous asymmetry quantified by the accumulation  $R_i$ . Through this strictly local adjustment, the constitutive geometry is continually refined until it supports local conservation. In this sense,  $W$  plays the role of a metric-like tensor on the graph, specifying how flux is measured and transmitted along each pathway. Conser-

vation is therefore enforced not by repeatedly applying a fixed operator, but by the continuous adaptive relaxation of the state along with the operator itself.

The remainder of this paper develops the formal structure of the HPN and demonstrates its operation on canonical transport problems. Section II defines the local fluxes and establishes that the Hebbian update constitutes a local gradient descent on the residual energy. Section III A examines scalar transport, illustrating how a consistent constitutive operator emerges solely through residual-driven feedback. Section III B extends the framework to incompressible lid-driven cavity flow, where pressure enforces the divergence constraint while the momentum-exchange weights adapt to maintain the correct local structure. Finally, in Section IV we discuss how physically consistent transport can arise from local constraint enforcement without a fixed operator. The HPN does not impose a constitutive geometry in advance; it learns one by continually adjusting the force-flux mapping so that imbalance is eliminated *in situ*.

## II. THERMODYNAMIC LEARNING VIA LOCAL RESIDUALS

Having established the qualitative framework of a ‘‘plastic’’ transport geometry, we now formalize the mechanics of adaptation. In this section, we define the HPN as a coupled dynamical system  $(U, W)$  and prove that the update rules are not arbitrary heuristics, but rigorous energy minimization procedures. We establish that while the weight update follows a biologically inspired Hebbian form (coupling local pre-synaptic state and post-synaptic accumulation), it mathematically constitutes a strictly local gradient descent on the residual energy. Furthermore, we demonstrate that near equilibrium, this plasticity naturally recovers the symmetric, linear transport laws predicted by Onsager’s reciprocity theory.

### A. Problem statement and notation

We consider a graph  $\mathcal{G} = (\mathcal{V}, \mathcal{E})$  with nodes  $i \in \mathcal{V}$  and directed edges  $(i, j) \in \mathcal{E}$ , such that  $i \rightarrow j$  and  $j \rightarrow i$  are distinct edges (see Fig. 1). Each node carries a  $d$ -component intensive state variable  $U_i \in \mathbb{R}^d$  ( $d=1$  for scalar transport;  $d=2, 3$  for planar or spatial fields). Each oriented edge carries a coupling operator  $W_{ij} \in \mathbb{R}^{d \times d}$ , representing the transport capacity (the geometric conductance) of that pathway.

To ensure physical consistency, we introduce a metric matrix  $\mathbf{G} = \text{diag}(\Omega_1, \dots, \Omega_N)$ , where  $\Omega_i > 0$  represents the local material parameters (e.g., density, viscosity, etc.) of node  $i$ . This metric ensures that the residual (an extensive quantity) is correctly mapped to the state update (an intensive quantity).

The directed flux along the edge is defined as:

$$J_{ij} = W_{ij} U_j. \quad (3)$$

For each node, we define the residual  $R_i$  as the **rate of accumulation** of the conserved quantity:

$$R_i(U; W) = \sum_{j \in \mathcal{N}(i)} J_{ij}. \quad (4)$$

Physically,  $R_i$  represents a local thermodynamic stress; if  $R_i \neq 0$ , the node is out of equilibrium.

To analyze the collective dynamics, we define the global state vector  $\mathbf{U} \in \mathbb{R}^{Nd \times 1}$  and the global residual vector  $\mathbf{R} \in \mathbb{R}^{Nd \times 1}$  as the concatenations of all nodal states and residuals.

## B. Thermodynamic Consistency of the Target Physics

We define the class of physical problems the HPN is designed to solve. We do not assume the network satisfies these properties *a priori*; rather, these are the properties of the target equilibrium that the network must discover.

**B1. Nature of the Conservation Law (Target Dissipativity):** The physical laws governing the residuals (e.g., mass or momentum balance) are assumed to be naturally dissipative. Mathematically, the symmetric part of the Jacobian of the ideal physics,  $\mathbf{L} = \partial \mathbf{R} / \partial \mathbf{U}$ , satisfies:

$$\mathbf{L}_{\text{sym}} = \frac{1}{2}(\mathbf{G}^{-1} \mathbf{L}^\top \mathbf{G} + \mathbf{L}) \succeq 0. \quad (5)$$

*Implication:* This restricts our scope to valid thermodynamic systems (excluding energy-generating singularities). It provides the “ground truth” energy landscape that the network attempts to learn.

**B2. Flux–Residual Alignment (Target Coercivity):** For the system to possess a stable attractor, the residual operator must be strictly monotone (coercive) near equilibrium.

$$\begin{aligned} (\mathbf{R}(\mathbf{U}_a) - \mathbf{R}(\mathbf{U}_b))^\top \mathbf{G}(\mathbf{U}_a - \mathbf{U}_b) \\ \geq c \|\mathbf{U}_a - \mathbf{U}_b\|_{\mathbf{G}}^2. \end{aligned} \quad (6)$$

For a positive constant  $c$ .

*Implication:* This corresponds to the Second Law’s requirement of strictly positive entropy production [10]. Unlike classical solvers that enforce this via fixed elliptic operators, the HPN may violate this condition transiently during adaptation. The goal of the learning dynamics is to recover this condition by reshaping the geometry.

## C. Constitutive Relaxation and the Onsager Limit

For scalar transport ( $d=1$ ), each edge carries a scalar weight  $w_{ij} \in \mathbb{R}$ . We now describe how this geometry adapts to stress.

*The Local Update Rule.* The local transport geometry evolves through a superposition of three mechanisms:

$$\Delta w_{ij} = - \underbrace{\eta_p f(R_i) U_j}_{\text{Penalty}} + \underbrace{\varepsilon g(|R_i|) U_j}_{\text{Promotion}} - \underbrace{\lambda w_{ij}}_{\text{Decay}}. \quad (7)$$

- The *Penalty* term drives the plastic deformation of the transport geometry. If a specific flux pathway contributes to local accumulation ( $R_i$  and  $U_j$  are correlated), this term reduces the effective geometric conductance of that edge. Conversely, if a pathway aids in relieving accumulation (anti-correlated), its conductance is increased.
- The *Promotion* term ensures non-vanishing transport capacity, maintaining a baseline permeability in the graph even near equilibrium.
- The *Decay* term imposes a physical bound on the coupling strength, preventing unbounded growth of the transport coefficients.

Without the promotion term, the update rule resembles the three-factor Hebbian rule as discussed in Eq. (2).

*Admissible modulators and Canonical Choice.* While the framework generally admits any  $f(\cdot)$  that is odd/monotone (with  $f(0) = 0$ ) and  $g(\cdot)$  that is bounded/decreasing, we specifically adopt the linear response  $f(x) = x$  and the exponential gate  $g(x) = \exp(-|x|)$  for the remainder of this work, making the weight update as follows:

$$\Delta w_{ij} = -\eta_p R_i U_j + \varepsilon e^{-|R_i|} - \lambda w_{ij}. \quad (8)$$

This choice is structurally preferred because, as we demonstrate below, the linear form  $f(R) = R$  is functionally equivalent local gradient descent and recovers the Onsager reciprocal relations near equilibrium.

*Gradient Descent Interpretation.* Consider the global residual energy  $\mathcal{L} = \frac{1}{2} \mathbf{R}^\top \mathbf{G} \mathbf{R}$ . The gradient with respect to a local weight  $w_{ij}$  is:

$$\frac{\partial \mathcal{L}}{\partial w_{ij}} = R_i \cdot \Omega_i \cdot \frac{\partial R_i}{\partial w_{ij}} = R_i \Omega_i U_j. \quad (9)$$

Comparing this to the plastic yield term in Eq. (8) (with absorbing  $\Omega_i$  into the learning rate) shows that the Hebbian update constitutes *local gradient descent* on the residual energy landscape. This ensures that even if the state dynamics are transiently unstable, the weight updates unconditionally minimize the local stress.

*The Onsager Limit (Proof of Reciprocity).* We now prove that near equilibrium, this adaptive framework naturally recovers the linear, reciprocal transport laws of standard thermodynamics.

1. **Stationarity Condition.** Consider the regime where weights have equilibrated ( $\Delta w_{ij} \approx 0$ ) and residuals are small ( $|R_i| \ll 1$ ). Using our defined forms

$f(R) = R$  and  $g(|R|) \approx g(0)$ , we solve Eq. (7) for the stationary weight  $w_{ij}^*$ :

$$\begin{aligned} 0 &= \varepsilon g(0)U_j - \eta_p R_i U_j - \lambda w_{ij}^* \\ \implies w_{ij}^* &= \frac{U_j}{\lambda} [\varepsilon g(0) - \eta_p R_i]. \end{aligned} \quad (10)$$

2. **Thermodynamic Flux Relation.** Substituting this stationary weight into the flux definition  $J_{ij} = w_{ij}^* U_j$ , we obtain:

$$J_{ij} = \underbrace{\frac{\varepsilon g(0)}{\lambda} U_j^2}_{J_{eq}} - \underbrace{\frac{\eta_p}{\lambda} U_j^2}_{L_{ij}} R_i. \quad (11)$$

The  $J_{eq}$  is the equilibrium flux, which can be considered zero. This equation allows us to identify the effective Onsager transport coefficient  $L_{ij}$  relating the restorative flux to the driving force ( $R_i$ ).

3. **Emergence of Reciprocity.** Crucially, in the near-equilibrium limit where spatial gradients are small ( $U_i \approx U_j$ ), these coefficients become symmetric:

$$L_{ij} = \frac{\eta_p}{\lambda} U_j^2 \approx \frac{\eta_p}{\lambda} U_i^2 = L_{ji}. \quad (12)$$

4. **Conclusion:** The Hebbian update naturally drives the system toward a symmetric transport operator ( $L_{ij} = L_{ji}$ ), reproducing Onsager reciprocity without explicit enforcement. The network self-organizes into a resistive medium where local conductance scales with the square of the local activity.

#### D. Lyapunov Dissipation Analysis

We now formally distinguish between the relaxation of the **state** and the relaxation of the **operator**. Let  $\mathcal{L} = \frac{1}{2} \sum_i \Omega_i R_i^2$ .

**Lemma 1** (State Dissipation / Onsager Process). *The state update  $\Delta \mathbf{U} \propto -\mathbf{G}^{-1} \mathbf{R}$  dissipates energy, provided the target coercivity condition (B2) holds locally:*

$$\Delta \mathcal{L}_{\text{state}} \leq 0. \quad (13)$$

*Proof.* By Taylor expansion,

$$\Delta \mathcal{L}_{\text{state}} = \mathbf{R}^\top \mathbf{G} \Delta \mathbf{R} = \mathbf{R}^\top \mathbf{G} \mathbf{L} \Delta \mathbf{U}.$$

Substituting

$$\Delta \mathbf{U} = -\gamma \mathbf{G}^{-1} \mathbf{R},$$

we get,

$$\Delta \mathcal{L} = -\gamma \mathbf{R}^\top \mathbf{L}_{\text{sym}} \mathbf{R} \leq 0.$$

Under Condition B1,  $\mathbf{L}_{\text{sym}} \succeq 0$ , ensuring dissipation.  $\square$

**Lemma 2** (Constitutive Dissipation). *For the weight update in Eq. (7) with strictly monotone  $f$ , the weight update is unconditionally dissipative:*

$$\Delta \mathcal{L}_{\text{weight}} \leq 0. \quad (14)$$

*Proof.*

$$\Delta \mathcal{L}_{\text{weight}} = \sum \frac{\partial \mathcal{L}}{\partial w_{ij}} \Delta w_{ij}.$$

Substituting the gradient (Eq. (9)) and the update rule (Eq. (8)) yields a quadratic form

$$-\eta_p \sum (R_i U_j)^2 \leq 0. \quad (15)$$

This holds regardless of whether Condition B2 is satisfied.  $\square$

*Physical interpretation:* Lemma 2 demonstrates that the plasticity acts as an unconditional ‘‘thermodynamic sink.’’ If C2 is transiently violated (instability in the flow), the resulting large residuals amplify the dissipative weight update, driving the system rapidly back toward a stable configuration.

#### E. Tensor Generalization and Energy Partition

For  $d > 1$ , edge operators  $W_{ij} \in \mathbb{R}^{d \times d}$  evolve via tensor updates. With  $\mathcal{L} = \frac{1}{2} \sum_i R_i^\top G R_i$ , the symmetric part of the tensor update dissipates energy ( $\Delta \mathcal{L}_{\text{sym}} \leq 0$ ) following the same gradient descent logic as the scalar case, while the skew-symmetric part organizes rotational transport without energy cost ( $\Delta \mathcal{L}_{\text{skew}} = 0$ ).

#### F. Dynamic Lyapunov Landscapes

Unlike fixed-operator energy networks, the HPN descends a *moving* Lyapunov landscape. Because the couplings adapt via gradient descent on the residual energy, the Lyapunov function  $\mathcal{L}(U; W)$  evolves *together with* the state.

- **Adaptive dissipation.** Node updates perform descent on the instantaneous energy. If the local geometry is ill-conditioned (C2 violated), weight updates reshape the manifold to restore the descent direction.
- **Operator coevolution.** As  $W$  adapts, the network maintains consistency between its current state and its constitutive geometry.

In this perspective, the Lyapunov landscape is a dynamic manifold shaped by local symmetry restoration. The symmetric component dissipates residual energy, while the skew component organizes flux without energy cost, resulting in a physically meaningful redistribution of imbalance.

### III. DEMONSTRATIVE CASES

To illustrate the scope of Hebbian Physics Networks (HPNs), we present two representative systems: incompressible flow in a lid-driven cavity and continuum diffusion. In both cases, physically consistent structures emerge from random or perturbed initial states through local residual relaxation and Hebbian weight adaptation—without explicitly solving the governing equations.

Throughout the remainder of this work, variables and parameters are reported in dimensionless form to facilitate scale-independent analysis. Unless explicitly stated otherwise, all quantities have been normalized by their respective characteristic values.

#### A. Diffusion

For diffusion on an unstructured graph with known connectivity, the continuity residual and directed flux are

$$R_{c,i} = - \sum_{j \in \mathcal{N}(i)} J_{ij}, \quad (16)$$

$$J_{ij} = DW_{ij}(c_j - c_i), \quad (17)$$

where  $c_i$  is the nodal concentration,  $W_{ij}$  is the weight associated with the directed edge  $j \rightarrow i$ , and  $D$  is the diffusivity. Classical graph-based discretizations prescribe  $W_{ij}$  directly from the geometric embedding (typically  $W_{ij} \propto \mathbf{r}_{ij}/\|\mathbf{r}_{ij}\|^2$ ) and treat it as fixed in time. Here, no geometric information is assumed *a priori*: the effective geometry is inferred through the learned weights  $W_{ij}$  themselves.

The node and weight updates follow the local Hebbian-residual rule

$$c_i^{n+1} \leftarrow c_i^n + \eta_c R_{c,i}^n, \quad (18)$$

$$W_{ij}^{n+1} \leftarrow W_{ij}^n + c_j^n \left( -\eta_w R_{c,i}^n + \varepsilon_w e^{-|R_{c,i}^n|} \right) - \lambda W_{ij}^n, \quad (19)$$

where the residual defines an eligibility,  $c_j$  acts as a modulatory signal, and the decay term ensures long-term boundedness of the couplings; superscripts,  $(\cdot)^n$ , represent the iteration index. The parameters used here are

$$\eta_w = 0.01, \quad \varepsilon_w = 0.001, \quad \eta_c = 0.001, \quad \lambda = 0.01.$$

The concentration field is initialized to zero, and a localized perturbation is introduced at  $n = 0$ ; all weights begin at unity.

Figure 2 summarizes the resulting dynamics. Panel (a) shows the evolution of the concentration field. The spreading front co-evolves with the operator: the fluxes (white quivers) are generated by  $W$ , and those fluxes in turn reshape  $W$  through the Hebbian update. This bidirectional coupling produces a finite-speed propagation of activity. The structure of the diffusion front in

panel (b)—obtained by tracking the  $y$ -coordinates of first activations—follows a clear parabolic envelope,  $r \propto \sqrt{n}$ , allowing the iteration index  $n$  to be calibrated against physical time.

The global residual in panel (c) exhibits an initial burst of fluctuations followed by rapid decay. The Lyapunov function  $\mathcal{L} = \frac{1}{2} \sum_i R_{c,i}^2$  in panel (d) decreases monotonically, demonstrating that each update constitutes a thermodynamically admissible local relaxation event. Panels (e) and (f) show the root-mean-square change in weights and the mean weight magnitude, respectively:  $W$  adapts substantially over the first  $\sim 4000$  iterations and then asymptotically freezes, marking the emergence of a stable constitutive operator. The histograms in panel (g) reveal the pruning behavior characteristic of the Hebbian rule: weights that do not contribute to residual reduction shrink toward zero, producing a bistable distribution that encodes the effective transport geometry of the learned medium.

Although the algebraic form of the update resembles a graph discretization of diffusion, the mechanism of evolution is fundamentally distinct from iterating the parabolic partial differential equation (PDE)  $\partial_t c = D\nabla^2 c$ . No global timestep is imposed, and no fixed Laplacian is ever constructed or inverted. Instead, both  $c$  and  $W$  evolve together:  $W$  determines the fluxes; the fluxes produce the residual; and the residual drives the joint update of the state and the operator. Each iteration is therefore not a step of a numerical solver but a *physical relaxation event* in which the network adjusts its internal geometry to reduce local imbalances. As  $W$  stabilizes, the emergent dynamics reproduce the diffusion law, but the system does not solve the PDE in the classical sense. The equilibration process itself—realized through adaptive local transport—is the computation.

#### B. Incompressible flow: lid-driven cavity

For incompressible flow we employ the Hebbian Physics Network in a hybrid form that separates *constraints* from *transport*. The Navier–Stokes operator is used only to evaluate the local momentum imbalance and the divergence of the velocity field; these quantities serve as physically faithful constraints that the learned transport operator must satisfy. The learning process itself does not attempt to reconstruct the Navier–Stokes operator, nor does it integrate the PDE in time. Instead, the network adapts a local interaction graph through which momentum is redistributed so as to reduce the residual implied by the constraint.

On a uniform grid with spacing  $h$ , the momentum and continuity residuals are computed using standard differential kernels,

$$\begin{aligned} R_u &= u \partial_x u + v \partial_y u - \partial_x p - \nu \nabla^2 u, \\ R_v &= u \partial_x v + v \partial_y v - \partial_y p - \nu \nabla^2 v, \\ R_c &= \partial_x u + \partial_y v, \end{aligned} \quad (20)$$

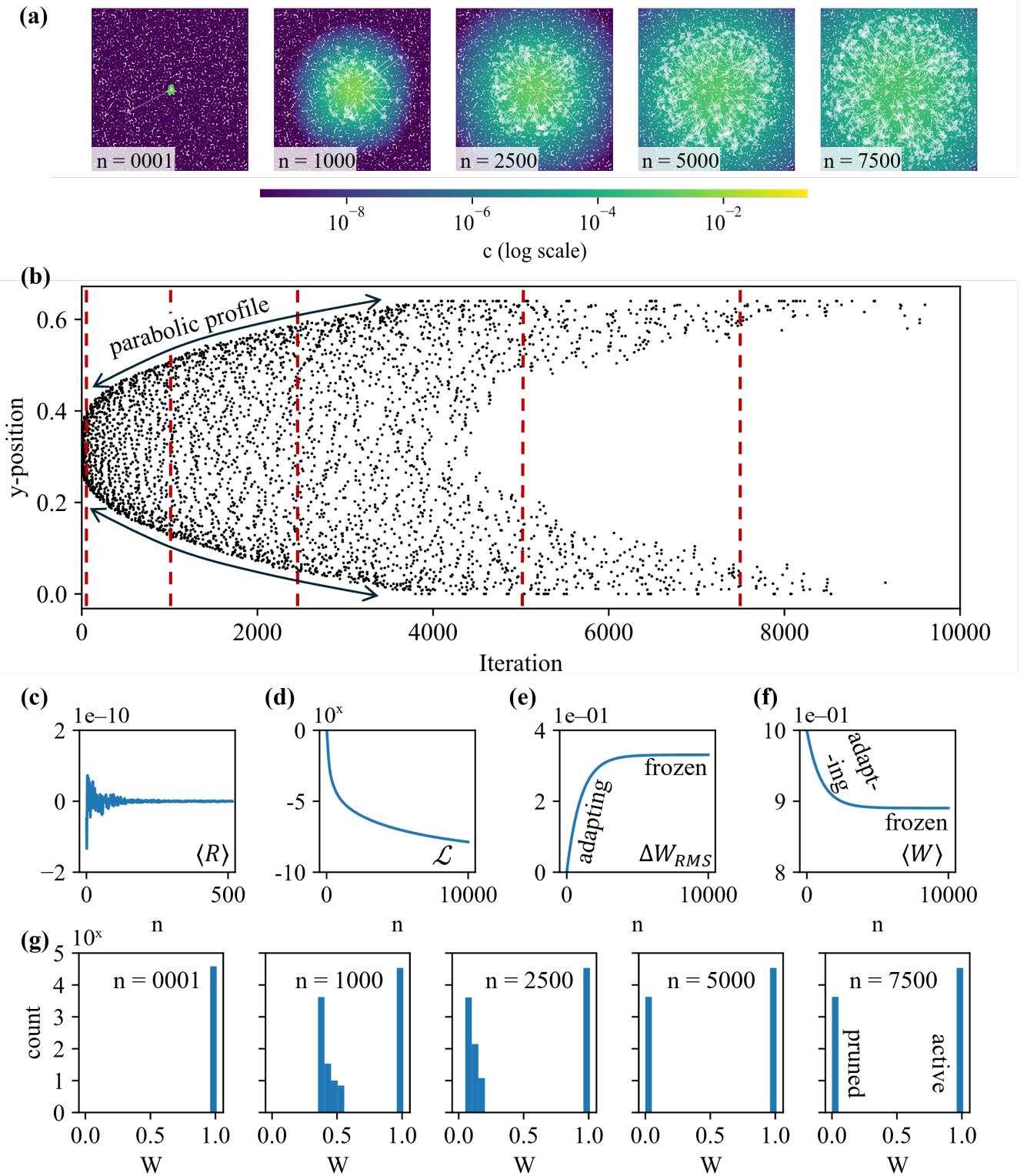


FIG. 2. **Residual-driven diffusion in a HPN** (a) Evolution of the concentration field on an unstructured graph. (b) Spatiotemporal trajectory of the diffusion front obtained by tracking the  $y$ -coordinates of nodes crossing a threshold concentration. Red dashed lines correspond to the iteration indices of the snapshots in (a). (c) Mean residual  $\langle R_c \rangle$  during relaxation. Fluctuations decay as local imbalances are removed by the Hebbian update. (d) Lyapunov function  $\mathcal{L}$  showing monotonic decrease with iteration. (e) Root-mean-square change in weights,  $\Delta W_{RMS}$ , indicating rapid early adaptation followed by asymptotic stabilization of the constitutive operator. (f) Mean weight magnitude  $\langle W \rangle$  approaching a steady value as the learned operator converges. (g) Histograms of the weight distribution  $W_{ij}$  at selected iterations.

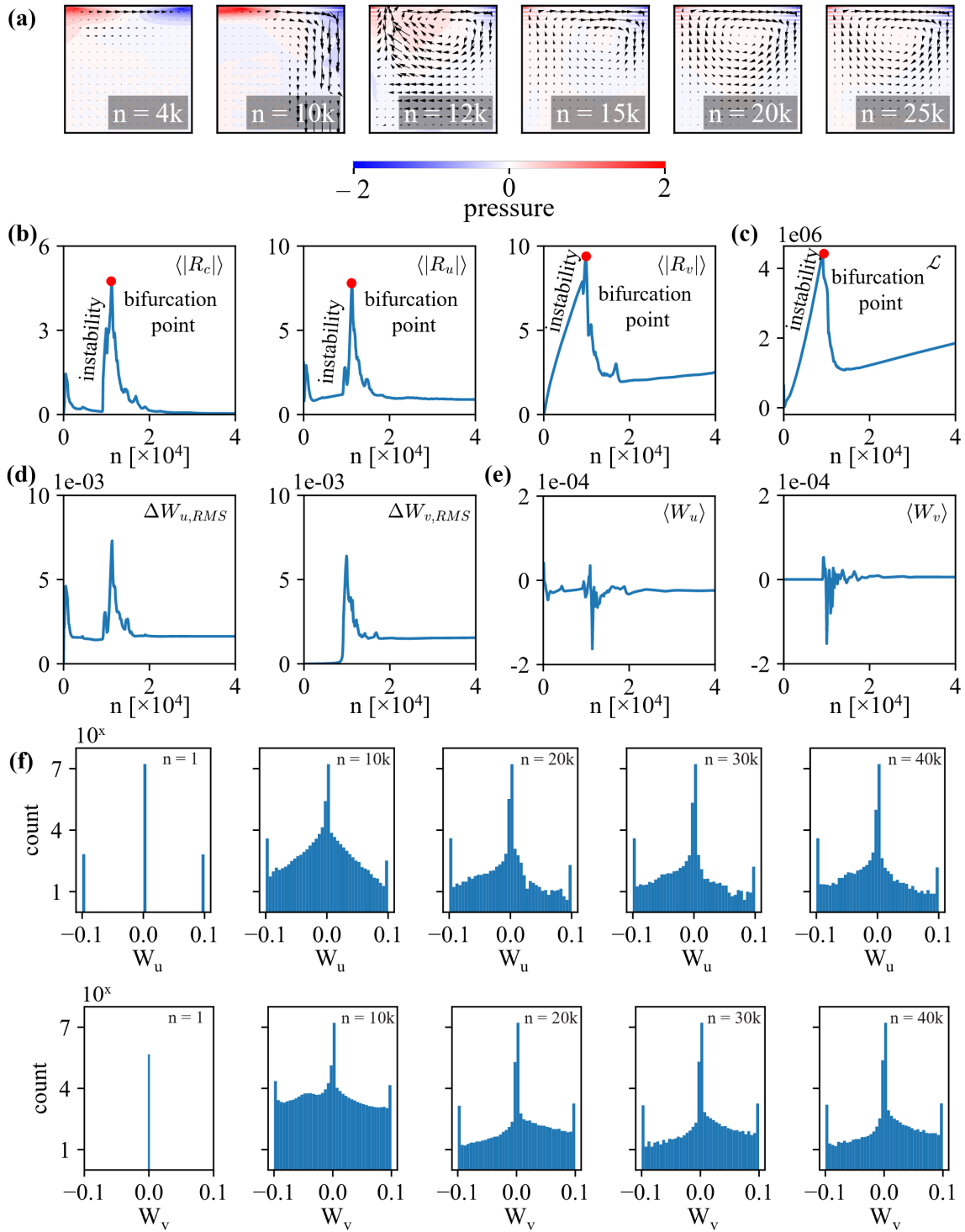


FIG. 3. **Residual-driven flow formation in a HPN.** (a) Streamline snapshots for the lid-driven cavity. From a nearly quiescent state, the network organizes the velocity into the characteristic recirculating pattern; pressure is shown as a background colormap, centered at zero. (b) Mean continuity, streamwise, and cross-stream residuals  $\langle |R_c| \rangle$ ,  $\langle |R_u| \rangle$ , and  $\langle |R_v| \rangle$ , showing an early surge followed by rapid decay as imbalances are redistributed through the learned transport operator. (c) Lyapunov function  $\mathcal{L} = \frac{1}{2} \sum_i (R_{c,i}^2 + R_{u,i}^2 + R_{v,i}^2)$ , increases until the networks “discovers” the vertical degree of freedom and bifurcates after reaching a maximum. (d) Root-mean-square weight changes  $\Delta W_{u,RMS}$  and  $\Delta W_{v,RMS}$ , indicating an initial phase of strong plasticity followed by stabilization. (e) Mean weights  $\langle W_u \rangle$  and  $\langle W_v \rangle$  approaching steady values as the transport geometry settles. (f) Histograms of  $W_{ij}^{(u)}$  and  $W_{ij}^{(v)}$  at selected iterations, initially narrow, then broadening during adaptation and developing heavy-tailed structure associated with shear, before converging as the flow reaches steady state.

where  $u$  and  $v$  are the velocity components,  $p$  is the pressure, and  $\nu$  is the viscosity. These fixed kernels are not treated as part of the learned dynamics; they define the physical consistency conditions that the network must relax toward at each iteration.

The relaxation dynamics are governed instead by two plastic weight matrices,  $W_u$  and  $W_v$ , which encode a local transport operator on a graph of radius  $k$  around each node. These weights evolve by a residual-driven three-factor Hebbian rule,

$$\begin{aligned} W_{u,ij}^{n+1} &\leftarrow (1 - \lambda) W_{u,ij}^n + u_j^n \left( -\eta_{wu} R_{u,i}^n + \varepsilon_w e^{-|R_{u,i}^n|} \right), \\ W_{v,ij}^{n+1} &\leftarrow (1 - \lambda) W_{v,ij}^n + v_j^n \left( -\eta_{wv} R_{v,i}^n + \varepsilon_w e^{-|R_{v,i}^n|} \right), \end{aligned} \quad (21)$$

so that couplings which help reduce the local residual are reinforced and those which oppose relaxation are suppressed. The velocity field is then updated by transport along the learned graph,

$$\begin{aligned} u^{n+1} &= u^n + \eta_u W_u^n u^n, \\ v^{n+1} &= v^n + \eta_v W_v^n v^n, \end{aligned} \quad (22)$$

followed by a pressure correction  $p^{n+1} = p^n + \eta_p R_c^n$  and enforcement of no-slip and moving-lid boundary conditions.

Figure 3 summarizes the relaxation dynamics of the Hebbian Physics Network applied to the lid-driven cavity. Panel (a) shows streamline snapshots at selected iterations. From an initially quiescent field, the flow organizes into the characteristic recirculating pattern as the learned transport operator redistributes momentum along locally imbalanced directions. The background pressure field, centered at zero, reflects the gradual establishment of the shear-driven pressure gradients, while the quiver arrows reveal the emergence and sharpening of the primary vortex. The oscillatory pressure features near the top corners do not indicate numerical instability. They arise from the local relaxation mechanism: without a global elliptic projection, the network enforces incompressibility through residual-driven adjustments that manifest as pseudo-acoustic pressure waves.

Panel (b) tracks the evolution of the residuals. The continuity residual  $\langle |R_c| \rangle$ , and the momentum residuals  $\langle |R_u| \rangle$  and  $\langle |R_v| \rangle$  in do not simply relax monotonically. Instead, they exhibit a pronounced initial surge followed by rapid decay. This surge is not a numerical artifact; it reflects a genuine dynamical phase transition in the residual-driven evolution. As the network begins enforcing the coupled incompressibility and momentum constraints, the imposed structure generates incompatible local stresses. These stresses accumulate until the system can redistribute them by reorganizing the transport operator and activating motion in the transverse direction. The sharp rise in residuals marks the onset of this instability, and the subsequent drop corresponds to the system settling into a regime in which

momentum can be redistributed consistently through the learned operator. The Lyapunov function in panel (c),  $\mathcal{L} = \frac{1}{2} \sum_i (R_{c,i}^2 + R_{u,i}^2 + R_{v,i}^2)$ , exhibits the same structure: an initial growth associated with the buildup of constraint-induced stress, followed by a relaxation trajectory once the reorganized operator provides an admissible pathway for reducing imbalance. Taken together, the evolution of the residuals forms a genuine dynamical bifurcation diagram for the early stages of the flow. The sharp peak—marked by the red point—corresponds to the bifurcation event at which the constraint-induced stress can no longer be accommodated within the initial operator structure, forcing the system into a new dynamical regime in which transverse momentum transport becomes active. This transition demonstrates that the HPN does not merely relax residuals, but is capable of identifying and adapting to distinct regions of the underlying dynamical landscape as the flow evolves.

Panel (d) displays the root-mean-square change in the weights  $\Delta W_{u,\text{RMS}}$  and  $\Delta W_{v,\text{RMS}}$ , showing an initial phase of strong plasticity as  $W$  responds to large residuals, followed by gradual freezing once the operator has adapted to the dominant shear and recirculation pattern. Panel (e) shows the mean weights  $\langle W_u \rangle$  and  $\langle W_v \rangle$ , which settle into steady values as the learned transport geometry stabilizes.

Panel (f) shows histograms of the weight distributions  $W_{ij}^{(u)}$  and  $W_{ij}^{(v)}$  at selected iterations. The initially narrow distributions broaden during the onset of flow formation, then develop a heavy-tailed structure aligned with regions of strong shear. As the steady vortex forms, weights that do not contribute to residual reduction shrink toward zero, while those aligned with active transport pathways remain reinforced. This pruning and anisotropic strengthening reflect the emergence of an effective constitutive transport operator tailored to the cavity flow.

This formulation identifies the local transport operator—rather than the Navier–Stokes operator itself—as the object to be learned. The fixed finite-difference kernels supply the momentum-balance and incompressibility constraints, while the evolving weights  $W$  determine how momentum is redistributed from one iteration to the next. In this sense the method is a controlled adaptation: the hydrodynamic residuals are defined by the standard operator, but the mechanism by which those residuals are relaxed is entirely learned. As the flow equilibrates, the transport operator develops clear flow-dependent structure—anisotropic in regions of strong shear, suppressed near solid boundaries, and organized around the primary recirculating vortex. These patterns reflect the effective pathways along which the network redistributes momentum to satisfy the constraints. Although the resulting velocity and pressure fields match the characteristic lid-driven cavity solution, the path taken to reach this state is not a numerical integration of the PDE; rather, the computation is the equilibration itself, mediated by a plastic local transport operator that continuously re-

shapes its geometry to resolve the imposed constraints.

## IV. DISCUSSION AND OUTLOOK

### A. Dynamic Theory: Local Symmetry Restoration and Adaptive Geometry

The Hebbian Physics Network (HPN) framework represents a class of dynamical systems that learn physical transport by suppressing local violations of conservation laws. Rather than descending a fixed global energy landscape, the dynamics proceed by reducing the residuals of mass, momentum, and related invariants within each neighborhood. This connects to the broader lineage of energy-based computation [11–13] and its non-equilibrium extensions [4, 6]. The essential point of departure is that, unlike classical networks with static couplings (dynamic only during training phase), HPNs evolve both the physical state and the local constitutive parameters concurrently. The system does not relax within a predetermined operator; it adapts the operator as part of the relaxation process. In this sense, the usual continuum equations appear as limiting descriptions of an underlying adaptive mechanism rather than as externally imposed governing laws.

The learned transport operator is defined globally by the sparse matrix  $\mathbf{W} \in \mathbb{R}^{N \times N}$ , but physically it functions as a dynamic geometric structure on the graph. We decompose the local interaction between any node pair  $i, j$  into two physically distinct components: a reciprocal component  $\mathbf{W}_{\text{sym}} = \frac{1}{2}(\mathbf{W} + \mathbf{W}^T)$  and a non-reciprocal component  $\mathbf{W}_{\text{skew}} = \frac{1}{2}(\mathbf{W} - \mathbf{W}^T)$ . The reciprocal component acts as an effective conductance metric, assigning bidirectional transport weights along edges and determining how strongly an imbalance propagates across each connection [14, 15]. Larger conductance corresponds to a locally “shorter” effective path for transport, while smaller conductance lengthens it. This component governs dissipative processes (e.g., diffusion, heat flow) where flux is driven down-gradient to maximize entropy production. The non-reciprocal component, by contrast, governs advective bias and local circulation; although energetically neutral, it plays a crucial role in organizing flow and redistributing imbalance through rotational mechanisms. This decomposition defines a discrete transport geometry:  $\mathbf{W}_{\text{sym}}$  determines dissipative alignment, while  $\mathbf{W}_{\text{skew}}$  structures solenoidal motion.

In practice, the Hebbian update modifies the raw weights  $W_{ij}$  and  $W_{ji}$  independently so that each node adjusts its local transport geometry until the residual it experiences is reduced to a sufficiently small value. Near equilibrium, as spatial gradients flatten ( $U_i \approx U_j$ ), the learning rule naturally converges to a symmetric configuration where the non-reciprocal component vanishes, recovering Onsager’s principle. Far from equilibrium, the system sustains a non-zero skew component to transport momentum across streamlines, stabilizing the flow

through advective redistribution. This process provides a concrete computational analogue of the way a locally inertial frame linearizes motion within a differential neighborhood [16, 17], though here the analogy reflects structure rather than physical curvature. For diffusive processes the effective metric adapts symmetrically; for incompressible flow the emergence of the non-reciprocal component reflects local circulation akin—at a discrete, algebraic level—to a torsion-like structure [18].

A consequence of this adaptability is that the relaxation pathway is not predetermined by the discretization. Conventional solvers follow a descent direction defined by a fixed operator. HPNs instead reshape this operator as they evolve, effectively reconditioning the local geometry of transport. This resembles a natural-gradient mechanism [14], where dynamics preferentially align with directions that most efficiently reduce imbalance. The ability to modify the transport geometry on the fly has potential implications for problems dominated by rare transitions [19, 20] or intermittent, structure-forming events in turbulence [21]: by adapting its local geometry, the network can straighten otherwise stiff directions of relaxation, potentially capturing events that require finetuned discretizations in fixed-operator solvers.

Overall, HPNs illustrate how local residual suppression can generate an adaptive constitutive geometry in which dissipation and operator formation occur together. This perspective suggests that classical PDEs may be viewed as coarse-grained, equilibrium-limit descriptions of a richer class of residual-driven adaptive processes. Future work will explore how this viewpoint scales to multiscale transport, turbulent flows, and systems with internal degrees of freedom.

### B. Local Constitutive Adaptation versus Global Enforcement

Conventional numerical solvers and physics-informed networks typically impose physical consistency through global procedures—solving a global constraint, minimizing a global loss, or enforcing variational optimality [22]. In contrast, HPNs embed consistency intrinsically. Each edge computes a flux proportional to the local imbalance, and each node measures the resulting divergence. The weights evolve through a three-factor Hebbian rule coupling residual, local state, and decay [23]. This implements a discrete analogue of the thermodynamic balance between force and flux [4]: residuals act as generalized forces, the local state modulates the response, and the decay term ensures that the overall dynamics remain dissipative.

Near equilibrium, the update reduces to a linear relation between fluxes and forces, recovering the familiar Onsager structure. Far from equilibrium, the nonlinear modulation of the update shapes the constitutive geometry while preserving Lyapunov admissibility. This perspective treats equilibrium not as a qualitatively different

regime but as a special limiting case of a single adaptive rule that governs both operator formation and relaxation.

A key distinction emerges relative to variational or optimization-based solvers. Those methods descend a loss defined by a fixed operator or fixed functional. HPNs, by contrast, update the constitutive geometry *during* the relaxation process itself: the system reorganizes the operator while suppressing the residuals that define consistency. Since the updates depend only on information within a finite neighborhood, the computational cost scales linearly with system size,  $\mathcal{O}(k^2N)$  for mean degree  $k$ .

### C. Physically grounded learning

We draw a motivating analogy from biological control. A bird navigating turbulent air does not compute the global Navier–Stokes equations. Mechanoreceptors provide local signals of pressure and shear, and the system adjusts coupling strengths (posture) to maintain stability [24–26]. The effective “transport operator” is thus learned in real time. The HPN framework formalizes this

principle: it maintains physical consistency by adapting local transport geometry in a manner akin to homeostatic feedback. The theoretical foundation developed here demonstrates that such constitutive-operator learning is empirically stable and consistent with classical transport processes in the tested regimes. Future work will rigorously quantify accuracy relative to established spectral solvers. Broadly, the HPN formalism frames computation as thermodynamic learning: systems compute by restoring local symmetry, providing a physically interpretable alternative to black-box optimization.

### ACKNOWLEDGMENTS

The open access publication of this work was supported by JSPS KAKENHI Grant Number JP23K28154 and JST CREST Grant Number JPMJCR24R2.

G.A. gratefully acknowledges his partner, Ms. Shambhavi Chaturvedi (National Institute of Genetics, Japan), for insightful discussions, especially on the neuroscience aspect relevant to this work.

- 
- [1] S. Patankar, *Numerical heat transfer and fluid flow* (CRC press, 2018).
  - [2] J. H. Ferziger, M. Perić, and R. L. Street, *Computational methods for fluid dynamics* (springer, 2019).
  - [3] R. J. LeVeque, *Finite volume methods for hyperbolic problems*, Vol. 31 (Cambridge university press, 2002).
  - [4] L. Onsager, Reciprocal relations in irreversible processes. i., *Physical review* **37**, 405 (1931).
  - [5] H. B. Callen, *Thermodynamics and an introduction to thermostatistics*, John Wiley& Sons **2** (1993).
  - [6] I. Prigogine and G. Nicolis, *Self-Organization in Non-Equilibrium Systems* (Wiley, 1977).
  - [7] I. Prigogine, Time, structure, and fluctuations, *Science* **201**, 777 (1978).
  - [8] N. Frémaux and W. Gerstner, Neuromodulated spike-timing-dependent plasticity, and theory of three-factor learning rules, *Frontiers in neural circuits* **9**, 85 (2016).
  - [9] L. Kuśmierz, T. Isomura, and T. Toyozumi, Learning with three factors: modulating hebbian plasticity with errors, *Current opinion in neurobiology* **46**, 170 (2017).
  - [10] S. R. De Groot and P. Mazur, *Non-equilibrium thermodynamics* (Courier Corporation, 2013).
  - [11] J. J. Hopfield, Neural networks and physical systems with emergent collective computational abilities, *Proceedings of the National Academy of Sciences* **79**, 2554 (1982).
  - [12] D. H. Ackley, G. E. Hinton, and T. J. Sejnowski, A learning algorithm for boltzmann machines, *Cognitive Science* **9**, 147 (1985).
  - [13] Y. LeCun, S. Chopra, R. Hadsell, M. Ranzato, F. Huang, *et al.*, A tutorial on energy-based learning, *Predicting structured data* **1** (2006).
  - [14] S.-I. Amari, Natural gradient works efficiently in learning, *Neural computation* **10**, 251 (1998).
  - [15] J. E. Marsden and T. S. Ratiu, *Introduction to mechanics and symmetry: a basic exposition of classical mechanical systems*, Vol. 17 (Springer Science & Business Media, 2013).
  - [16] C. W. Misner, K. S. Thorne, and J. A. Wheeler, *Gravitation* (Macmillan, 1973).
  - [17] V. I. Arnold, *Geometrical methods in the theory of ordinary differential equations*, Vol. 250 (Springer Science & Business Media, 2012).
  - [18] F. W. Hehl, P. Von der Heyde, G. D. Kerlick, and J. M. Nester, General relativity with spin and torsion: Foundations and prospects, *Reviews of Modern Physics* **48**, 393 (1976).
  - [19] H. A. Kramers, Brownian motion in a field of force and the diffusion model of chemical reactions, *physica* **7**, 284 (1940).
  - [20] C. Dellago, P. G. Bolhuis, F. S. Csajka, and D. Chandler, Transition path sampling and the calculation of rate constants, *The Journal of chemical physics* **108**, 1964 (1998).
  - [21] U. Frisch and A. N. Kolmogorov, *Turbulence: the legacy of AN Kolmogorov* (Cambridge university press, 1995).
  - [22] M. Raissi, P. Perdikaris, and G. E. Karniadakis, Physics-informed neural networks: A deep learning framework for solving forward and inverse problems involving nonlinear partial differential equations, *Journal of Computational Physics* **378**, 686 (2019).
  - [23] D. O. Hebb, *The organization of behavior: A neuropsychological theory* (Psychology press, 2005).
  - [24] W. R. Ashby, *An introduction to cybernetics* (Chapman & Hall, 1956).
  - [25] R. E. Brown and M. R. Fedde, Airflow sensors in the avian wing, *Journal of experimental biology* **179**, 13 (1993).

- [26] R. Pfeifer and J. Bongard, *How the body shapes the way we think: a new view of intelligence* (MIT press, 2006).